Whitmarsh, R.B., Sawyer, D.S., Klaus, A., and Masson, D.G. (Eds.), 1996
Proceedings of the Ocean Drilling Program, Scientific Results, Vol. 149

40. DYNAMIC MODELS OF MULTIPHASE CONTINENTAL RIFTING AND THEIR IMPLICATIONS FOR THE NEWFOUNDLAND AND IBERIA CONJUGATE MARGINS[1]

David L. Tett[2] and Dale S. Sawyer[2]

ABSTRACT

Rifting between Newfoundland and Iberia occurred in two distinct phases—the first late Triassic to Early Jurassic, the second Late Jurassic to Early Cretaceous—culminating in the creation of the North Atlantic Ocean. A dynamic modeling method is used to examine the implications of multiple phases of rifting on the development of the Newfoundland-Iberia conjugate margins.

A set of models based roughly on the Newfoundland and Iberian Margins suggests that, under most conditions in which two rift phases occur, the site of the original rift will not be favored for extension when stretching resumes, because the upper mantle cools and strengthens in the area of the original rift. The models predict a lack of magmatism on these margins and suggest that extension was significantly greater in the second rifting phase than in the first; these predictions agree with geological observations. The models do not predict the existence of highly thinned continental crust on both conjugate margins, however.

INTRODUCTION

Where Newfoundland and Iberia separated to form part of the North Atlantic Ocean, there is evidence for two phases of rifting, with an intervening tectonically quiet phase. Ocean floor creation did not begin until after the second phase of rifting successfully broke North America and Iberia apart. The driving forces of rifting appear to have stopped for a period of time on these margins. What implications did such a tectonic "resting phase" have for the rifting history as well as the features observed today on the Newfoundland and Iberian Margins?

To attempt to answer this question, we employed a dynamic modeling method used most recently by Harry and Sawyer (1992a, 1992b). We devised a set of models that incorporates the resting phase. This contrasts with existing models, which are based on a single event (e.g., Dunbar and Sawyer, 1989; Chéry et al., 1990; Keen and Boutilier, 1990; Bassi, 1991; Harry and Sawyer, 1992a, 1992b; Bassi et al., 1993).

We begin by briefly reviewing the Mesozoic rifting history of the Newfoundland and Iberian Margins. We follow with an examination of the consequences of multiphase rifting in a set of generic models based roughly on the Newfoundland and Iberian Margins. Finally, we propose a model that approximates the crustal thickness and subsidence profile and the patterns of extension of the Newfoundland and Iberian Margins.

DESCRIPTION OF THE NEWFOUNDLAND-IBERIA CONJUGATE MARGINS

The Newfoundland and Iberian Margins are similar. Each margin contains two sets of basins: one landward of the continental shelf break and the other seaward of the shelf break. Thus, four basin sets form the conjugate margins. They are, from west to east, the basins of the Grand Banks of Newfoundland, Newfoundland Basin, Iberia Abyssal Plain, and Lusitanian Basin.

The Grand Banks is a 450-km-wide continental shelf off Newfoundland (Tankard and Welsink, 1987) with an average water depth of less than 200 m (Welsink et al., 1989). The Grand Banks is underlain by continental crust between 32 and 38 km thick (Tankard and Welsink, 1987, 1989; Reid and Keen, 1990).

The Newfoundland Basin extends about 200 km to the southeast from the Grand Banks continental slope (Tucholke et al., 1989). Its bathymetry ranges from 2000 to 5000 m, but averages about 4000 m. This basin contains between 2 and 7 km of sediments (Tucholke et al., 1982, 1989). Many workers (Tucholke et al., 1989; Austin et al., 1989; Sullivan, 1983; Masson and Miles, 1984; Meador and Austin, 1988) have interpreted most of the crust under the Newfoundland Basin to be highly extended continental crust with a thickness of 4 to 8 km (Tucholke et al., 1989), with the ocean/continent boundary at the "J anomaly" (Pitman and Talwani, 1972; Tucholke and Ludwig, 1982; Malod and Mauffret, 1990; Srivastava et al., 1990; Austin et al., 1989). This interpretation is not universally accepted (Parson et al., 1985); several authors (Keen and de Voogd, 1988; Malod and Mauffret, 1990) place the ocean/continent boundary closer to the shelf break, implying that the crust underlying the Newfoundland Basin is oceanic. In our efforts here, we attempted to model this crust as extended continental crust.

The Iberia Abyssal Plain lies seaward of the narrow Iberian continental shelf and is about 350 km wide. Water depth ranges from 3000 to more than 5000 m, crustal thickness appears to be 5 to 8 km, and sediment thickness is 1 to 3.5 km (Whitmarsh et al., 1990). As in the Newfoundland Basin, the location of the ocean/continent boundary is uncertain, but may coincide with a ridge of serpentinized peridotite that parallels the Portuguese coast (Boillot et al., 1987). Whitmarsh et al. (1990, 1993) proposed that much of the Iberia Abyssal Plain is underlain by thinned continental crust, based on its seismic velocity structure and a magnetic model.

The Lusitanian Basin is completely underlain by continental crust with a thickness of about 30 km (Banda, 1988; Cordoba et al., 1988; Whitmarsh et al., 1990). The basin parallels the Portuguese coast, and is more than 250 km long and 50 to 100 km wide. The part of the basin landward of the Iberia Abyssal Plain lies onshore; it was uplifted

[1]Whitmarsh, R.B., Sawyer, D.S., Klaus, A., and Masson, D.G. (Eds.), 1996. *Proc. ODP, Sci. Results,* 149: College Station, TX (Ocean Drilling Program).

[2]Department of Geology and Geophysics, Rice University, MS 126, 6100 South Main St., Houston, TX 77005-1892, U.S.A. (Tett, present address: Amoco Worldwide Exploration Business Group, P.O. Box 3092, Houston, TX 77253, U.S.A.) dltett@amoco.com

primarily because of compression related to Pyrenean and Alpine mountain building (Wilson et al., 1989). (Please note that while some [e.g., Murillas et al., 1990] assert that the Galicia Interior Basin to the north is an offshore continuation of the Lusitanian Basin, the analyses performed in the research documented here concern only the portion of the Iberian Margin in the direct vicinity of the Iberia Abyssal Plain, from about 39°30'N to 41°N latitude.) Sediment thickness varies from 0 to 4 km in the Lusitanian Basin (Wilson et al., 1989).

The evidence indicates that rifting progressed from south to north (Srivastava et al., 1988; Murillas et al., 1990). Extensional structures were localized along Avalonian and Hercynian crustal weaknesses (Keen et al., 1987; Tankard and Welsink, 1989). Rifting began in the Carnian (235 Ma) in the Lusitanian Basin (Wilson et al., 1989; Leinfelder and Wilson, 1989) and in the Grand Banks basins (Tankard and Welsink, 1987); this phase of extension ended at about 210 Ma. (Absolute ages are based on Harland et al., 1990.)

A period of thermal subsidence followed on both margins. At about 160 Ma, extension was renewed on the Grand Banks (Tankard and Welsink, 1988; Tankard et al., 1989; Grant et al., 1988; Keen et al., 1990) and in the Lusitanian Basin (Wilson, 1975; Montenat et al., 1988; Leinfelder and Wilson, 1989; Murillas et al., 1990; Hiscott et al., 1990; Mauffret and Montadert, 1987) and was most intense through about 150 Ma.

Extension became more concentrated in the zone of the future ocean/continent boundary in the Early Cretaceous. Extension had begun in the Newfoundland Basin (Tucholke et al., 1989; Austin et al., 1989) and in the Iberia Abyssal Plain (Whitmarsh et al., 1990; Montenat et al.,1988) by 140 Ma. During the final 20 m.y. or so of rifting, there was little additional extension in the shelf basins of both margins. By the end of the Barremian (124 Ma), creation of oceanic crust had begun, and rapid subsidence in the seaward basins occurred; a breakup unconformity (the Avalon unconformity in the basins of the Grand Banks) marked this event (Murillas et al., 1990; Groupe Galice, 1979). Serpentinized peridotite was emplaced on the Iberian Margin at the ocean/continent boundary (Boillot et al., 1987), and although no evidence has been found of it, perhaps on the Newfoundland Margin as well. In general, then, the earlier phase of rifting was limited to the shelf basins, whereas the later phase was marked by a shift in extension from the shelf basins to the deep-water basins, culminating in seafloor spreading.

Masson and Miles (1986) provided a possible explanation for this pattern of rifting. During the late Triassic phase of rifting, Iberia moved with Africa, so that extension took place simultaneously between the eastern United States and Africa and between Newfoundland and Iberia. After 195 Ma, a transform boundary developed between Iberia and Africa and along the southern margin of the Grand Banks, allowing Africa and North America to continue rifting and finally to separate (at about 175 Ma), while little or no extension occurred between Newfoundland and Iberia (Masson and Miles, 1986; Tankard and Welsink, 1988). Srivastava and Verhoef (1992) suggested that, during this period, the southern Grand Banks high was dragged away from the rest of the Grand Banks by Africa. After 160 Ma, extension resumed again between these margins and progressed to the point of continental breakup and seafloor spreading. Srivastava et al. (1990) indicated that Iberia was moving as a separate plate when spreading began. (Ziegler, 1989, provides a well-illustrated map-view history of Mesozoic North Atlantic rifting.)

Little rift-related magmatism is observed on either side of the Atlantic. The central Newfoundland Basin is dotted by the mid-Cretaceous Newfoundland Seamounts, but these are unrelated to the rifting of these margins. Also, aside from some dike intrusion in southeastern Newfoundland during the Early Jurassic and some minor volcanic rock found in wells, rift-related igneous activity is scarce on the Grand Banks (Keen et al., 1990; Tankard and Welsink, 1988). Mesozoic magmatism in the Lusitanian Basin is insignificant (Montenat et al., 1988).

The conjugate margins display mild asymmetries. Figure 1 shows a cross section of the margins, perpendicular to the direction of rifting. The Iberia Abyssal Plain appears to be slightly wider than the Newfoundland Basin (350 vs. 200 km); this probably indicates that the site of seafloor spreading was somewhat off-center in a broad area of highly extended crust. In addition, the subsidence amounts for the Iberia Abyssal Plain and the Newfoundland Basin (labelled "TTS" in Fig. 1) are somewhat different (Tett, 1993). These asymmetries are limited to the highly thinned areas adjacent to the ocean/continent boundary, however, and are minor if the margins are considered as a whole. Figure 1 also may give the impression that basement underlying the Iberia Abyssal Plain is rougher; this difference merely reflects the levels of detail in the data shown in this figure. The observed subsidence profile is compared to the modeled subsidence in Figure 15.

Lastly, the continental shelf on the Newfoundland margin (not shown in Fig. 1) is 1 order of magnitude wider than that on the Iberian side; at first glance, this variance seems to be a significant asymmetry. Much of the Grand Banks, however, is the unextended Bonavista platform (Srivastava and Verhoef, 1992), and the Iberian shelf has become emergent largely because of Cenozoic compression. Thus, although the *basins* are wider on the Grand Banks than the Lusitanian Basin, the asymmetry of the shelf widths is not as extreme as the bathymetries would suggest.

These observations notwithstanding, the Newfoundland and Iberian Margins are grossly symmetric. During both phases of extension, rifting was distributed symmetrically through time on both margins, first on the shelf basins, and later in the more seaward basins. Common lithologies are found on both sides of the Atlantic throughout the rifting history. In addition, the two phases of extension were centered in the same location, so that the resulting conjugate margins are roughly mirror images of one another.

DYNAMIC MODELING METHOD

To model the extension of continental lithosphere, we used the finite-element method (FEM) originally employed by Dunbar and Sawyer (1988, 1989) and also by Harry and Sawyer (1992a, 1992b). (A more complete treatment of the modeling method can be found in these papers.) In this method, a vertical slice of the lithosphere was represented as a two-dimensional thermomechanical continuum, approximated by a "mesh" of elements.

The deformation of the model was governed by two different empirically determined rheological laws. The yield stress of each element was computed using Byerlee's (1978) law frictional sliding and also using a power law viscous creep of the form

$$\dot{\varepsilon} = A\,\sigma^{n} \exp(-Q_c/RT). \quad (1)$$

The value for yield stress actually used for each element at each time step was the lower of the values predicted by these two laws, because deformation most likely occurs by the mechanism that requires the least stress. The temperature, pressure, strain rate, and lithology all influence the deformation mechanism for which the yield stress is least.

Brittle faulting in the upper crust was approximated by ideal plasticity, and no deformation by discrete faulting occurred in the model. Thus, although the formation of individual fault-controlled basins was not computed, the *overall* extension in the upper crust was estimated. The FEM included neither sedimentation nor any magmatic process such as partial melting. The FEM included, however, the effects of buoyancy forces, the model's own flexural strength, and the weight of any overlying seawater. The driving forces of plate tectonics, and continental lithospheric extension in particular, were approx-

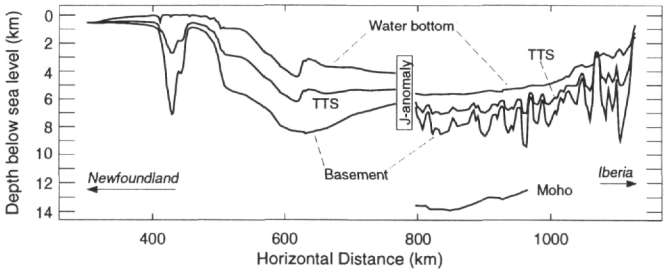

Figure 1. Cross section of the Newfoundland and Iberia Abyssal Plain conjugate margins, showing basement depth, water depth, total tectonic subsidence (TTS), and Moho depth (where observed). Horizontal distance is arbitrary and is meant only for scale. The narrow basin at about 400 km is the Jeanne d'Arc Basin. The shorelines of Newfoundland and Iberia are just off the figure to the left and right, respectively. Newfoundland Margin data were digitized from maps by Tucholke et al. (1982) and Tucholke and Fry (1985); Iberian Margin data were digitized from a profile by Whitmarsh et al. (1993). The two profiles are reconstructed to depict the J anomaly interpretation of the ocean/continent boundary location.

imated by constant-velocity boundary conditions on the sides of the model (Keen, 1985; Kusznir and Ziegler, 1992; Ziegler, 1992).

The FEM included heat generation in the crust; the amount of heat generated per unit volume decreased exponentially with depth. The top of the model was kept at 0°C throughout the model run. At the bottom of the model lithosphere, a constant heat flow (e.g., Braun and Beaumont, 1989a, 1989b) was maintained. (The method used to calculate the heat-flow values is described below.) We chose this boundary condition because we were interested in modeling the effect of a "resting phase" on the pattern of extension; the conductive cooling of extended lithosphere during this phase would have occurred too slowly, if at all, if a constant-temperature bottom boundary condition (e.g., Braun and Beaumont, 1987) had been chosen.

The bottom-temperature boundary condition was determined in the following manner. The unextended initial model was allowed to equilibrate thermally with a temperature of 0°C at the top and 1333°C at the bottom of the model. The vertical temperature gradient across the bottom row of elements was multiplied by the mantle conductivity to arrive at the vertical heat flow. Because the lithospheric thickness—in effect, the distance separating the 0° and 1333°C isotherms—could vary horizontally across the model, so did the thermal gradient; hence, the heat flow could vary laterally across the model as well. These heat-flow values were used as the bottom boundary condition for the remainder of the model run.

It must be noted that the constant heat-flow boundary condition will probably permit the lithosphere to cool too quickly. This boundary condition does not allow upwelling asthenosphere to become part of the lithosphere, an event that we think may have occurred during rifting of the Newfoundland-Iberian Margins. The modeling routine employed here offered only two choices of bottom boundary condition—constant temperature and constant heat flow—and modifying the code to model the thermal regime more accurately was outside the scope of the research described here. In cases of prolonged or interrupted rifting, we believe that the choice of constant heat flow is clearly the more accurate of the two options.

The modeling routine also lacks the blanketing effects of sedimentation. If sediments, which generally have low conductivity, had been included in the thermal model, the cooling of the lithosphere would have occurred at a slower rate, and thus the patterns of rifting may have been different. We are unsure of the implications of this model feature on our results; nevertheless, the conclusions of this paper still hold true for the thermal regimes used.

The continental lithosphere was represented by three rock types and their associated rheological properties (Table 1). The model mantle was wet Aheim dunite (Chopra and Paterson, 1981). Two

Table 1. Creep law rheological parameters used in the models presented.

Rheological parameters:	A	Q_c	n	r
	($Pa^{-n}\ s^{-1}$)	kJ $mole^{-1}$		kg m^{-3}
Wet aheim dunite	4×10^{-25}	498	4.5	3300
Wet quartz diorite	5×10^{-18}	219	2.4	2850
Wet granite	8×10^{-16}	137	1.9	2670

Note: These parameters were used in the formula $\dot{\varepsilon} = A\sigma^n \exp(-Qc/RT)$ to determine the stress at each node in the model mesh.

lithologies were used to model continental crust: wet quartz diorite (Hansen and Carter, 1982) represented typical continental crust and wet granite (Hansen and Carter, 1983) represented weakened continental crust. These rheologies had been used previously by Harry and Sawyer (1992a) to model the rifting lithosphere. We did not investigate the effect of using different rheologies on multiphase rifting. The thermal properties listed in Table 2 were also used in all models.

DESCRIPTION OF THE GENERIC MODEL SUITE

The intent of this lithospheric modeling experiment was to test the response of initial models with different lithospheric weaknesses to extension through different multiphase extension "paths." In this paper, we present only certain models that illustrate our conclusions. First, however, a description of the full "generic" model suite follows.

Each model was initially 800 km long and underwent 500 km of extension over the duration of the model run. These values are estimates of extension across the Newfoundland and Iberian Margins (Tett, 1993). (These values reflect our supposition that the crust underlying the Newfoundland Basin and the Iberia Abyssal Plain is of continental affinity.) Each model was run for 120 m.y., which was approximately the length of time from the beginning of the first rifting phase (about 230 Ma) to the initiation of seafloor spreading (about 110 Ma) on the Newfoundland-Iberia conjugate margins. All of the generic models were symmetrical.

It should be noted at this point that the 110 Ma date for continental breakup is based on an unconformity found at Deep Sea Drilling Program (DSDP) Site 398 at the Aptian/Albian boundary (Groupe Galice, 1979)—about 110 Ma. This unconformity may reflect the breakup on the nearby Galicia Margin to the north, however. This date was intended only to approximate the date of initial seafloor spreading on these margins and, as will be seen below, was not used in designing the more margin-specific model.

Rifting "Paths"

Although all models had the same total amount of extension over the same total duration of time, they had different instantaneous extension rates during that interval. Over its 120-Ma span, each model had one rifting rate for the first 25 Ma, a different rate for the next 45 Ma, and yet another rate for the final 50 Ma. These durations were chosen because they approximate the durations of the first (late Triassic) rifting phase, the resting phase, and the second (Late Jurassic to Early Cretaceous) rifting phase on the Newfoundland-Iberian Margins. Each sequence of extension rates for the three phases was called a rifting "path."

Five different rifting paths were used (Table 3, Fig. 2). The extension rate (and hence the amount of extension) for the middle phase was zero in paths 1, 2, 3, and 5; this represented the period in which there is thought to have been no divergent motion between North America and Iberia (about 215 to 160 Ma). The paths were intended to simulate different distributions of the total extension between the first and second rifting phases. Path 4 is a constant extension rate for the entire duration of rifting.

Table 2. Thermal parameters used in the models presented.

Thermal parameter	Value
Crustal heat production	
Surface heat production	3×10^{-6} W m^{-3}
Exponential decay depth	10 km
Conductivity	
Crust	2.5 W m^{-1} °K^{-1}
Mantle	3.4 W m^{-1} °K^{-1}
Specific heat	
Crust	875 J kg^{-1} °K^{-1}
Mantle	1250 J kg^{-1} °K^{-1}
Coefficient of thermal expansion	3.1 x 10^{-5} °K^{-1}
Asthenosphere density	3189 kg m^{-3}

Table 3. Description of the rifting paths used in the generic model suite.

Rifting Paths	Path number				
	1	2	3	4	5
Phase 1: 0–25 Ma					
Extension rate (km Ma^{-1})	0	2	6	4.17	10
Percent of total extension during this phase	0	10	30	20.8	50
Amount of extension during this phase (km)	0	50	150	104	250
Phase 2: 25–70 Ma					
Extension rate (km Ma^{-1})	0	0	0	4.17	0
Percent of total extension during this phase	0	0	0	37.5	0
Amount of extension during this phase (km)	0	0	0	188	0
Phase 3: 70–120 Ma					
Extension rate (km Ma^{-1})	10	9	7	4.17	5
Percent of total extension during this phase	100	90	70	41.7	50
Amount of extension during this phase (km)	500	450	350	208	250

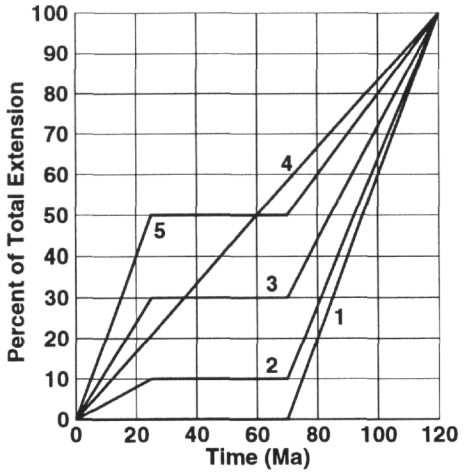

Figure 2. Rifting paths (1 through 5) used in the generic set of models. The vertical axis indicates the cumulative percentage of total extension; horizontal axis indicates time since the beginning of rifting. The total amount of extension in each generic model is 500 km. The slope of each line is proportional to relative rate of extension.

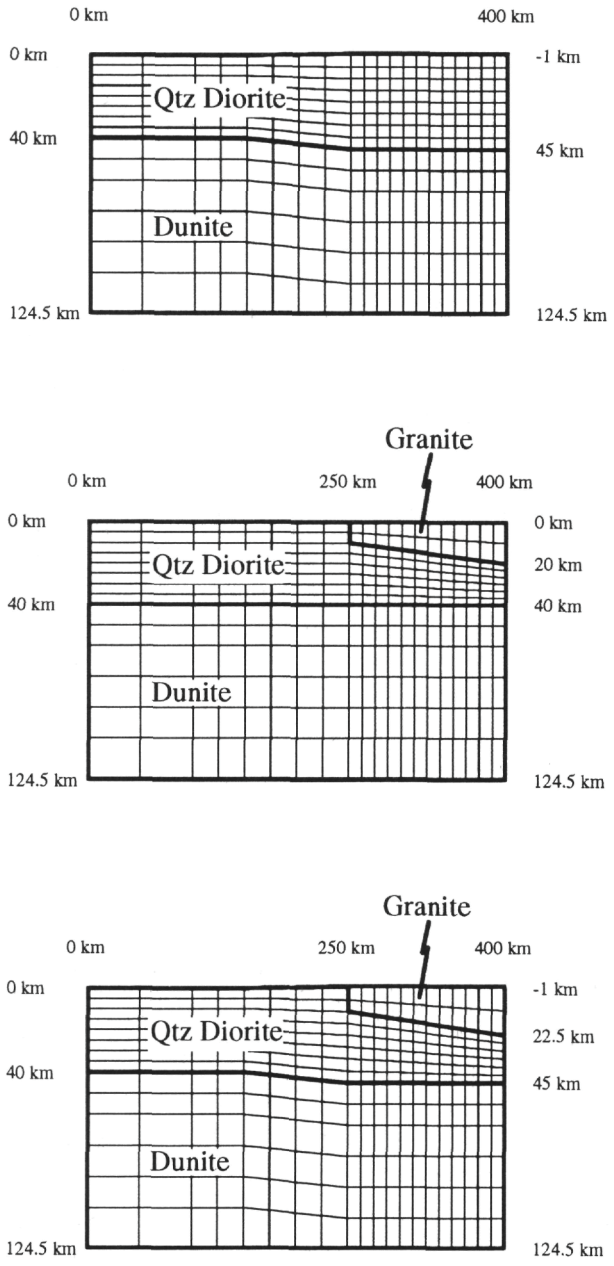

Figure 3. Initial models "MW" (mantle weakness only), "CW" (crustal weakness only), and "BS" (both crustal and mantle weaknesses), from top to bottom, respectively.

Initial Models

Three different initial models were tested, each of which contains a different type of lithospheric weakness. The weakness types were taken from Dunbar and Sawyer (1989).

The first initial model, "MW," contains a mantle weakness, formed by a section of crust 5 km thicker than the flanking "normal thickness" crust (Fig. 3). The crust in this model was represented entirely by a quartz diorite rheology. In the models considered here, the mantle and lower crust lie mainly in the ductile field, where yield strength varies inversely with temperature (Fig. 4). At identical temperatures, the quartz diorite rheology is much weaker than the dunite rheology. Hence, where a crustal welt replaced mantle dunite with crustal quartz diorite in a model, the vertically integrated strength of a column of lithosphere was lowered.

The second initial model, "CW," contains a crustal weakness (Fig. 3). Here, a section of quartz diorite crust was replaced with the wet granite rheology. The thickness of this weakness ranged from 10 to 20 km. The CW initial model is weakened by the same amount as model MW (Fig. 4).

The third initial model, "BS" (both symmetric), contains both a mantle and a crustal weakness, which are symmetrical about the same point (Fig. 3). The sizes of the weaknesses were the same as in the individual MW and CW models, although in the BS model the crustal

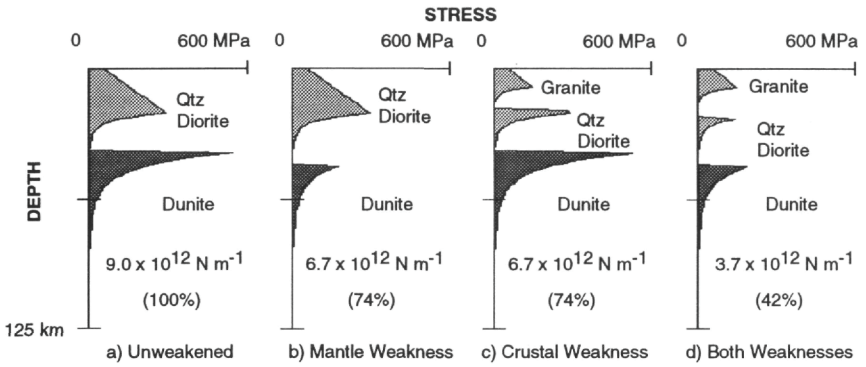

Figure 4. Initial strength profiles of the model lithosphere. Flow stress is calculated from empirical steady-state creep relations at a constant strain rate of 10^{-15} s^{-1}, with the maximum stress limited by Byerlee's (1978) frictional failure criterion. **A.** Profile of normal, unweakened lithosphere. **B-D.** Profiles through initial models MW, CW, and BS, respectively. The total strength (integrated stress) and relative strength of the lithosphere are indicated near the bottom of each curve.

weakness made up 25% to 50% of the crust, independently of the crustal thickness. The BS model is quite a bit weaker than the previous two initial models (Fig. 4).

Stretching the three different starting models using five different extension paths produced 15 models in total.

RESULTS OF THE GENERIC MODEL SUITE

The mechanical meshes of a few of the 15 models are shown in Figures 5, 6, 7, and 9. For models following path 4, the steps shown are roughly equally spaced (in the time domain) from beginning to end. For paths 3 and 5, we show the beginning, middle, and end of both the first and the second rifting phases. Note that, for these paths, the mesh at the end of the first rifting phase (25 Ma) is roughly the same as the mesh at the beginning of the second (70 Ma), because between these two times, no extension was applied to the models. Keep in mind that these models represent one-half of a symmetrical rifting margin. For clarity, after each model name in the text and figure captions we list in parentheses the percentages of total extension for each phase.

The following conclusions were drawn from the generic model suite:

Temperature and Locus of Extension

At any point in time, the upper mantle extension will localize where the Moho is hottest. For the power law creep rheology, strength is inversely related to temperature; cooling the mantle only a little will greatly strengthen it. In the models in which mantle extension migrates laterally, cooling is sufficiently fast relative to the rate of extension that the upper mantle becomes stronger than the neighboring hotter (and weaker) mantle. Because the upper mantle is the strongest portion of a vertical slice of lithosphere in most cases, when the upper mantle strength decreases, the strength of the entire lithosphere decreases. Indeed, the mantle weakness becomes a mantle *strength* once it cools sufficiently, preventing further significant extension at that location. This increase in strength from cooling is the same phenomenon presented by England (1983) and discussed most recently by Bassi et al. (1993). This effect is also similar to the phenomenon proposed by Steckler and ten Brink (1986), in which rifting in the Red Sea region was directed away from the previously thinned (and thus stronger) Mediterranean continental margin. In the models presented here, however, the phase of extension affected by earlier rifting occurs relatively soon after the original episode and is roughly parallel to the original orientation of rifting. The upper mantle may become shallow enough to enter the brittle failure regime (Sawyer, 1985), but it still remains stronger than neighboring hotter mantle. It is this strengthening of the zone of initial rifting that causes the locus of extension to move laterally outward from the center of the model. This effect would be diminished in cases where heavy sedimentation reduces the cooling rate, but is nonetheless present in instances of lighter sedimentation (as our model represents).

This behavior is exhibited by many of the generic models, where the locus of extension migrates laterally. In model MW4 (20.8, 37.5, 41.7), the rate of extension is slow enough to allow the mantle in the center to cool and strengthen and cause a shift in necking location (Fig. 5). Necking begins in the center of this model, but the locus of necking moves closer to the edges of the model as time progresses; extension is roughly evenly distributed across the original mantle weakness. This mesh looks very similar to the "runaway thinning" model presented by Bassi et al. (1993).

In model MW3 (30, 0, 70), the second phase of rifting occurs at the outer flanks of original wide weakness, where the Moho is deepest and hottest (Fig. 6). The center of the model stretches a bit more in the second phase, but by the end of the second phase, necking on the flanks of the original mantle weakness has taken over.

During the first phase, model CW5 (50, 0, 50) necks more in the center then the aforementioned models, because the most extension is assigned to the first phase in this path (Fig. 7). At 25 Ma, strain is concentrated entirely in middle of the model. At the beginning of the second rifting phase, the upper mantle is extremely cold and strong at the center, and the necking shape created in the first phase is practically frozen (Figs.7, 8). Figure 8 shows that the strain rate is extremely low in the center of the model throughout the second phase of rifting; the area of highest strain rate always stays about halfway between the model's center and its outer edge. The strain rate is fairly high even at the outer edge of the model.

Role of Crustal Weakness

The location of crustal weaknesses will be the initial location of crustal extension. Once the mantle lithosphere becomes sufficiently thinned at a different location, however, crustal thinning will proceed there. Early during extension, the crustal weakness (with a granite lithology) is partly in the ductile deformation regime and is thus weaker than the surrounding quartz diorite crust. As the crustal weakness is necked and cools, it enters the brittle deformation field entirely. Because Byerlee's (1978) law is insensitive to rock type, the granite crustal weakness is no longer weaker than the neighboring "normal" quartz diorite crust. Once the crust becomes equally strong everywhere, crustal deformation is controlled by the location of upper mantle strain, and hence the entire lithosphere begins to strain at the same location.

Model BS4 (20.8, 37.5, 41.7) exhibits such a migration of crustal extension (Figs. 9, 10). In this mesh, both crustal and mantle extension are more evenly distributed throughout the model; this difference is probably the result of the relatively low extension rate. In the strain rate plot in Figure 10, the area of highest mantle strain rate moves from center outward; the strain rate decreases more slowly in the crust at the center than in the mantle. Extension is always more diffuse in the crust, and produces pervasive shear just above the Mo-

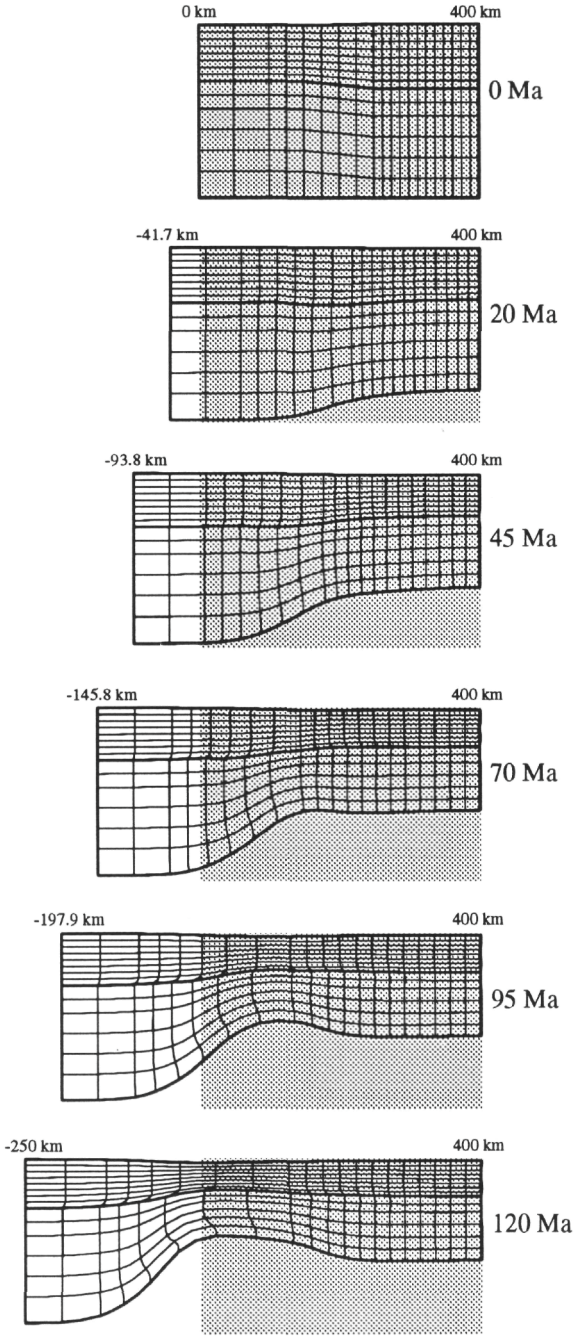

Figure 5. Deformation of the mechanical mesh for model MW4 (20.8, 37.5, 41.7). The gray box represents the size of the initial model (400 km wide by 124.5 km deep) at each time step.

ho. (This lower crust shear provides a "reasonable" mechanism for decoupling crust and mantle stretching, which Rowley and Sahagian [1986] claimed was lacking in previous nonuniform stretching models.) It is clear that, at each time from 70 Ma onward, the highest strain rate occurs in a location slightly outward from the most highly necked area (Fig. 10); this mechanism allow the locus of necking to migrate outward. The phenomenon of the mantle weakness controlling the later stages of rifting is a similar result to that reached by Harry and Sawyer (1992a).

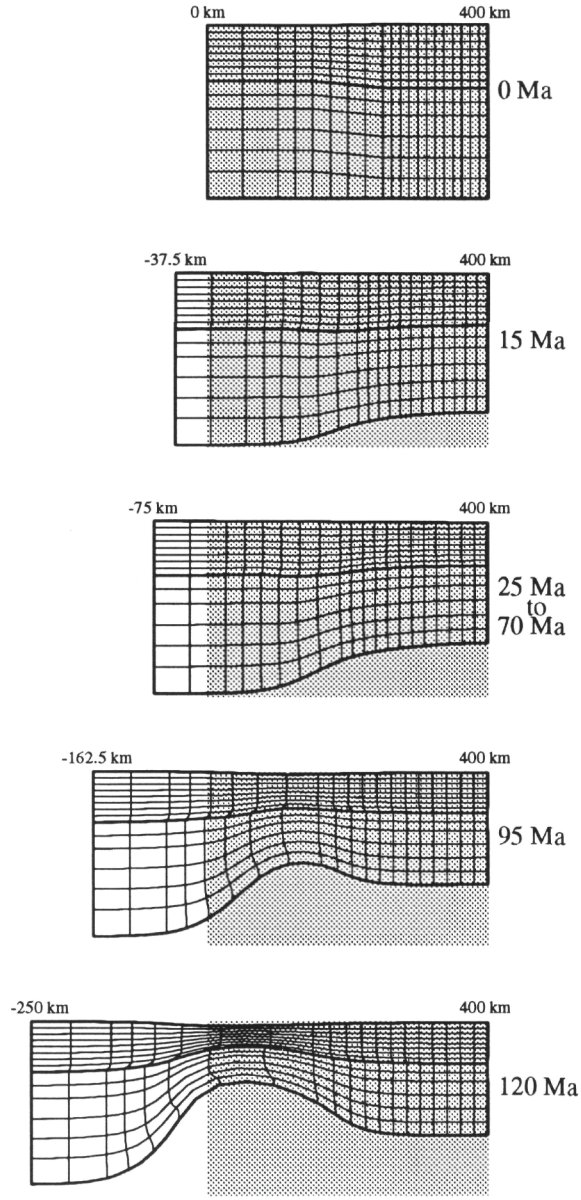

Figure 6. Deformation of the mechanical mesh for model MW3 (30, 0, 70). The gray box represents the size of the initial model (400 km wide by 124.5 km deep) at each time step.

Effect of a Resting Phase

These models suggest that the occurrence of a resting phase between two episodes of rifting should greatly affect the morphology of a continental rift. In most cases, the site of the original rift will *not be* favored for extension when stretching begins anew. If extension in the first phase is significant, the crust will be thinned and the Moho elevated. During the resting phase, the upper mantle will cool and strengthen. When rifting begins anew in the second phase, the original site of rifting will be a lithospheric strong zone, and second-phase rifting will occur in a different, weaker location. Furthermore, a resting phase (or other variation through time in the rate of rifting) could serve as a possible explanation for areas where the location of rifting is observed to migrate through time. While the temperature boundary

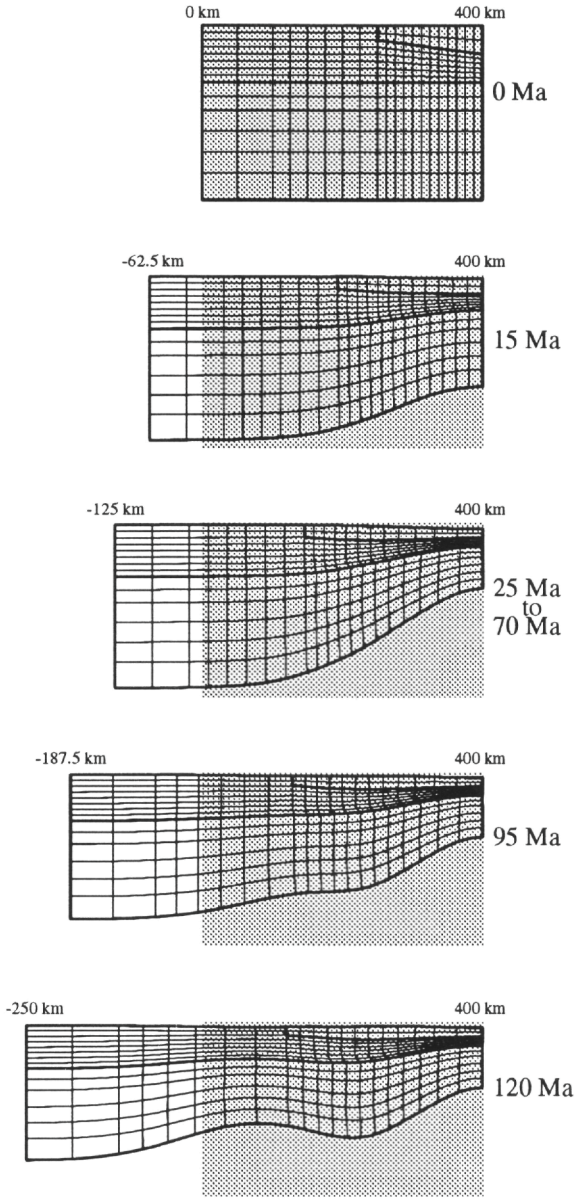

Figure 7. Deformation of the mechanical mesh for model CW5 (50, 0, 50). The gray box represents the size of the initial model (400 km wide by 124.5 km deep) at each time step.

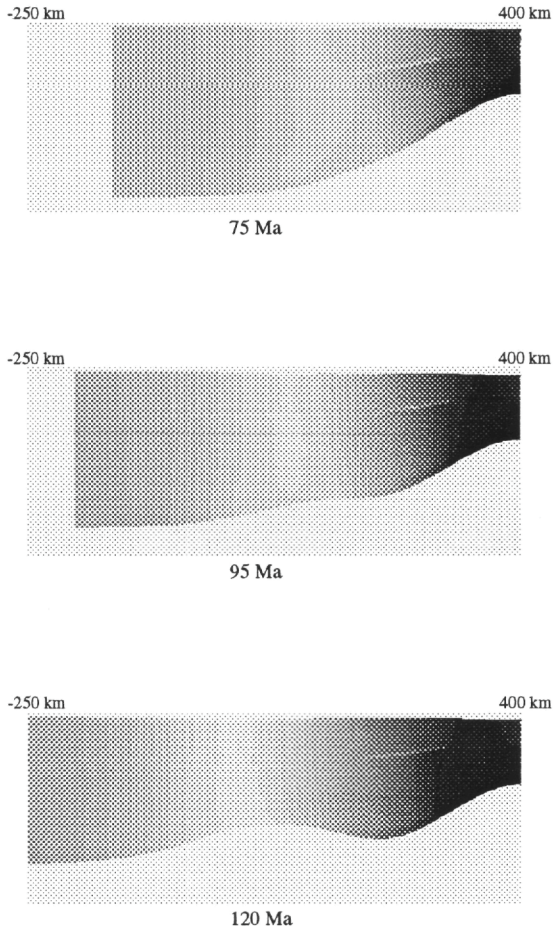

Figure 8. Strain rate plot for model CW5 (50, 0, 50). Grays range from $\log_{10}$ (strain rate) of -14.9 (black) to -12.4 (white). The light background delineates the maximum width (650 km) and original thickness of the model (124.5km).

conditions presented here probably represent the "cooler end" of the spectrum of possible rifting thermal regimes, we do not feel that the thermal conditions are unreasonably cool. Of the models in the generic model suite, model MW3 (30, 0, 70) demonstrates this phenomenon the best (Fig. 6).

DESIGNING A MORE MARGIN-SPECIFIC MODEL

Based on the conclusions of the generic models, we attempted to design a model that more closely approximated the rifting history of the Newfoundland-Iberia conjugate margins. The generic model suite results suggest that, if the first phase of extension were significant, the second phase of extension would occur at a different location. Because the second rift phase on these margins occurred in roughly the same place as the first, we infer that the first phase of extension must have been sufficiently minor not to create a strong zone in the lithosphere and shift the second phase of rifting elsewhere.

We aimed to approximate only the gross lithospheric features of the Newfoundland and Iberian Margins. Primarily, we were interested in reproducing the crustal thickness profile across the two margins. On the Canadian side, the crust is 35 to 38 km thick across the Grand Banks and thins gradually seaward of the Jeanne d'Arc Basin to an ultrathin 4 to 8 km beneath the Newfoundland Basin. On the Iberian side, the crust on the continent is about 30 km and thins gradually to 5 to 8 km over a broad area. We tried to model the crustal profile, as well as the distribution of upper crust extension and subsidence.

The original width of the model and the amount of extension it underwent were based on values estimated for the Newfoundland and Iberian Margins (Tett, 1993); for simplicity, we rounded the original width to 600 km and the amount of extension to 400 km. (As in the generic models, these parameters reflect our supposition of a continental nature of Newfoundland Basin and Iberia Abyssal Plain crust.) Of that 400 km, we assigned 60 km to the first rifting phase and 340 km to the second. This choice was based on the value of $\beta = 1.1$ that Hiscott et al. (1990) cited for the Triassic sequences of the Bristol Channel area and in the Wessex Basin in the British Isles. Although we are uncertain of the method by which this figure was estimated, and even though it applies to the British basins and not the ones ex-

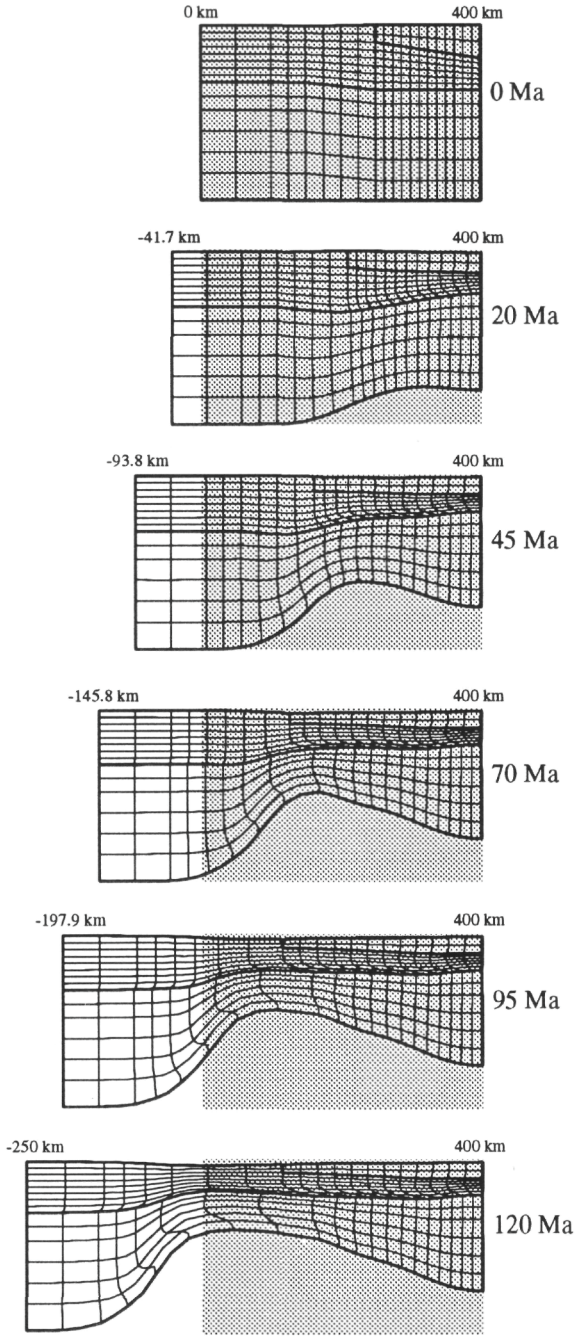

Figure 9. Deformation of the mechanical mesh for model BS4 (20.8, 37.5, 41.7). The gray box represents the size of the initial model (400 km wide by 124.5 km deep) at each time step.

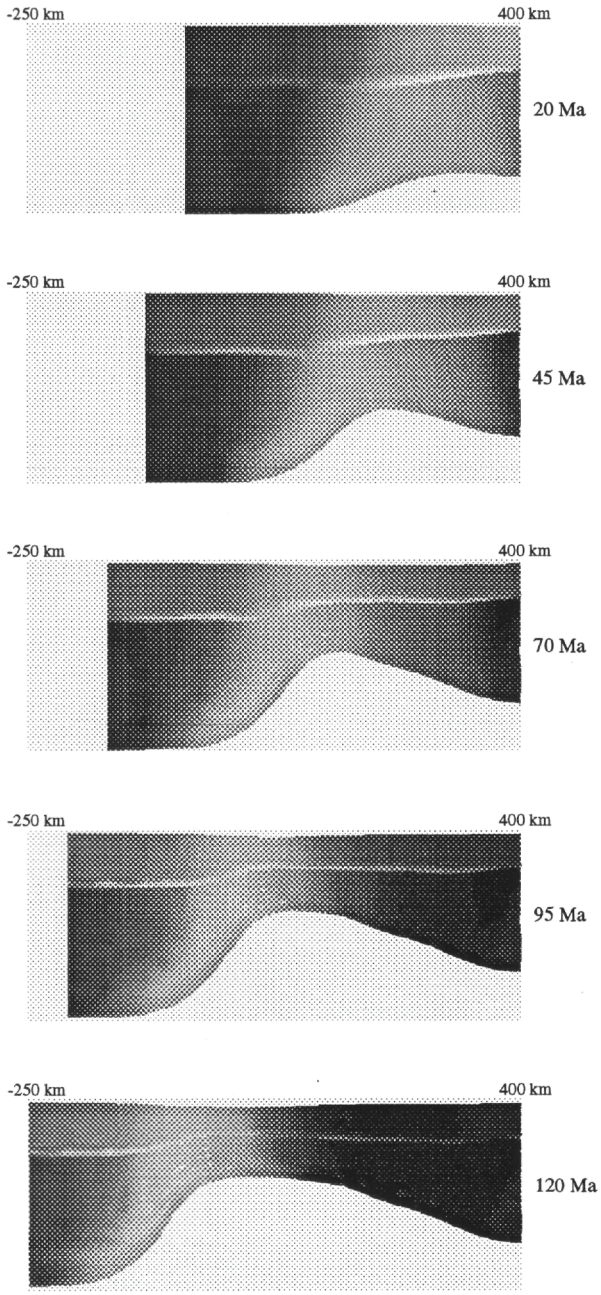

Figure 10. Strain rate plot for model BS4 (20.8, 37.5, 41.7). Grays range from $\log_{10}$ (strain rate) of -14.9 (black) to -11.4 (white). The light background delineates the maximum width (650 km) and original thickness of the model (124.5 km).

amined in this paper, it is the best estimate available. Paleomagnetic data cannot resolve the amount of extension between Iberia and North America (J.E.T. Channell, pers. comm., 1993). The upper Triassic synrift sediments of the Newfoundland and Iberia shelf basins are buried so deeply, and salt tectonics have deformed the sediments so extensively, that reliable estimates of extension for the Triassic are difficult to obtain.

We assigned durations (25 and 45 Ma, respectively) to the first rifting phase (which lasted roughly from 230 to 205 Ma) and the resting phase (which lasted from 205 to 160 Ma) that are similar to those used in the generic model suite. We chose a duration of 35 Ma (instead of 50 Ma) for the second rift phase, however, using the following reasoning. The second phase is though to have begun at about 160 Ma. Our preliminary choice of 110 m.y. for the initiation of seafloor spreading yielded a duration of 50 Ma for the second phase of the generic model suite. Because a date of 125 Ma is a more accurate average date for the rift-drift transition on the transect discussed here, we reduced the estimate of second-phase duration to 35 Ma. (This had the net effect of making the second phase of rifting faster, making less likely a shift in locus of extension.) The choices for distribution and duration of extension during the two rifting phases results in the rifting path shown in Figure 11. The extension rate of 9.7 km/m.y. (half-rate of 4.85 mm/yr) for the second phase is significantly less

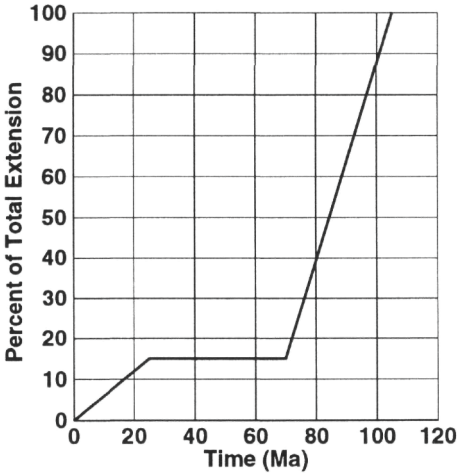

Figure 11. Rifting path used for the margin-specific model. Vertical axis indicates the cumulative percentage of total extension; horizontal axis indicates time since the beginning of rifting. The total amount of extension is 400 km, and the total duration of extension is 105 Ma. The slope of line is proportional to relative rate of extension.

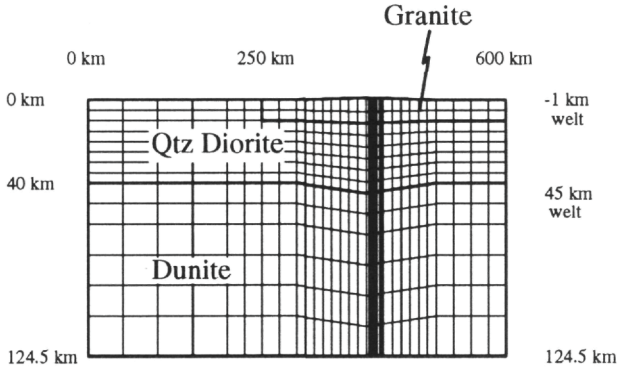

Figure 12. Initial model for the Newfoundland-Iberia conjugate margins.

than the rate of initial seafloor spreading on the southern half of the Newfoundland margin (24 to 26 km/m.y.; half-rate of 12 to 13 mm/yr) given by Srivastava et al. (1990). Although this discrepancy is somewhat discouraging, it must be remembered that the extension rate used here is an average over a period of 35 Ma, whereas the initial seafloor-spreading rate is an instantaneous one. Though it is not included in our model, it is conceivable that the instantaneous rate of extension increased during the second phase of rifting, resulting in an average rate quite a bit lower than the rate of rifting just before seafloor spreading.

Several parameters for the initial model (Fig. 12) are less well constrained. The original crustal thickness is almost impossible to constrain. The crust beneath Newfoundland itself, in the heart of unextended Appalachian orogen, ranges in thickness from 40 to 45 km. The Paleozoic orogen was enormously complex, and the part of the orogen about which we are most concerned has been obliterated by extension. Lacking any independent constraints on the original crustal thickness profile, we chose original crustal thicknesses between 40 and 46 km.

The crustal weakness in the model (Fig. 12) was chosen with a similar level of speculation. It was designed to mimic the distribution of the rift basins on the continental shelves of the Newfoundland and Iberian Margins. The shelf basins nucleated on weaknesses inherited from different orogenies on both sides. On the Iberian side, the Porto-Badajoz-Cordoba shear zone (PBCZ)—the major Paleozoic transform fault in western Iberia (Lefort, 1989)—became the eastern boundary of the Lusitanian Basin and served as the landward limit of extension. In southeastern Newfoundland, a similar major strike-slip fault, the Dover fault, appears to be the PBCZ's counterpart on the opposite margin (Keen et al., 1986) and would seem to be a location favored for upper crust extension. Basins on the Newfoundland margin, however, nucleated on Precambrian Avalonian weaknesses, hundreds of kilometers seaward of the Dover fault. Thus, it is impossible to attribute with any certainty a single factor that controlled the upper crustal basin formation, and hence that could be chosen as a "crustal weakness" in the margin-specific model. The role of any crustal weakness is a major uncertainty in the model.

The width and location of the crustal welt (the mantle weakness) in the initial model (Fig. 12) are speculative as well. Without exception, attempts to design a model with a wide crustal welt led to "wide rifting"—a style that we do not think is manifested on these conjugate margins. To achieve the narrow rifting style that appears to have occurred here, we had to use a narrow mantle weakness. The position of the crustal welt in the model reflects the estimates of original margin width (Tett, 1993); the Newfoundland Margin (to the left) is designed to be much wider than the Iberian (to the right). Also, the location of shelf basins and the crustal profile indicate a predominantly symmetrical rifting style. Attempts to model these margins using a model with moderate to large asymmetry resulted in extremely poor fits to the observed crustal profile. Thus, the weaknesses in the initial model are roughly symmetrical.

RESULTS OF THE MARGIN-SPECIFIC MODEL

The lithosphere stretches very little in the first phase (Fig. 13), and the root of the original orogen is removed, but further crustal thinning does not occur at the site of the mantle weakness. The Moho beneath the original crustal welt started with a higher temperature than the adjacent Moho. Although the upper mantle cools during the resting phase, this temperature difference is preserved, and by the beginning of the second rift phase at 160 Ma (+70 Ma, Fig. 13), the Moho beneath the area of first-phase necking still has a higher temperature than the neighboring Moho. Thus, the lithosphere is weakest there, and second-phase necking concentrates in the same place as first-phase extension. Necking continues at the same place until 130 Ma (+100 Ma). After this time, the mesh becomes so deformed that the FEM becomes unstable, and the model does not execute its last time step (125 Ma). Nevertheless, the mesh is sufficiently necked there to assume that, in the final time step, necking would be concentrated there.

Before 145 Ma, the strain rate is distributed in a manner similar to that shown at 145 Ma in Figure 14. Between 145 and 135 Ma, however, necking rapidly concentrates at the location of highest strain (Fig. 14). This timing is consistent with the shift of extension from the Grand Banks and Lusitanian Basin (on the shelves) to the Newfoundland Basin and Iberia Abyssal Plain at about 140 Ma.

The elevation on the Iberian side of the model does not match the subsidence values computed for the Iberia Abyssal Plain margin (Fig. 15) (Tett, 1993). Nevertheless, the abrupt change in slope between 100 and 200 km on the profile resembles the shape of the shelf break on the Newfoundland Margin, and the slope of the model's surface between 150 and 350 km is similar to the continental slope on the Newfoundland Margin. Although the model elevation will drop further owing to thermal subsidence—rendering the fit poorer—the shape of the Newfoundland Margin is predicted by this model.

Similarly, the crustal profile of the model fits the actual crustal thickness reasonably well on the Canadian margin, but poorly on the Iberian side. None of our attempted models—including the final one shown here—features broad zones of highly thinned crust, as are observed on both conjugate margins.

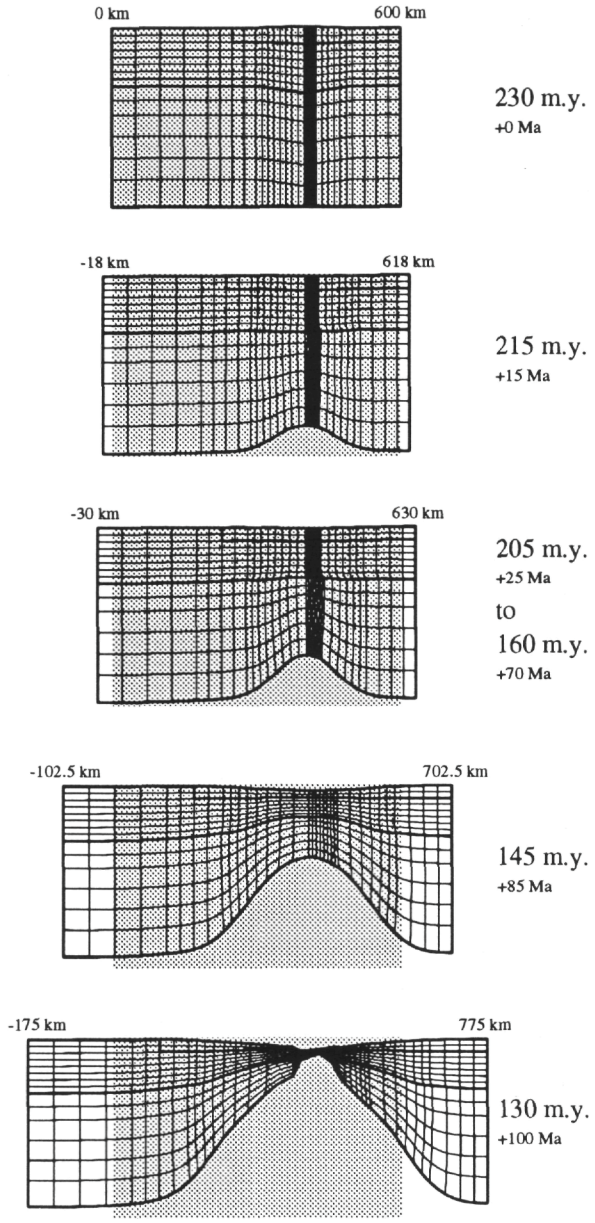

Figure 13. Deformation of model mechanical mesh. The larger date to the right of each mesh indicates the geologic date in millions of years before present; the smaller date indicates time since the start of the model and corresponds with the time scale of the generic models. The gray box represents the size of the initial model (600 km wide by 125 km deep) at each time step.

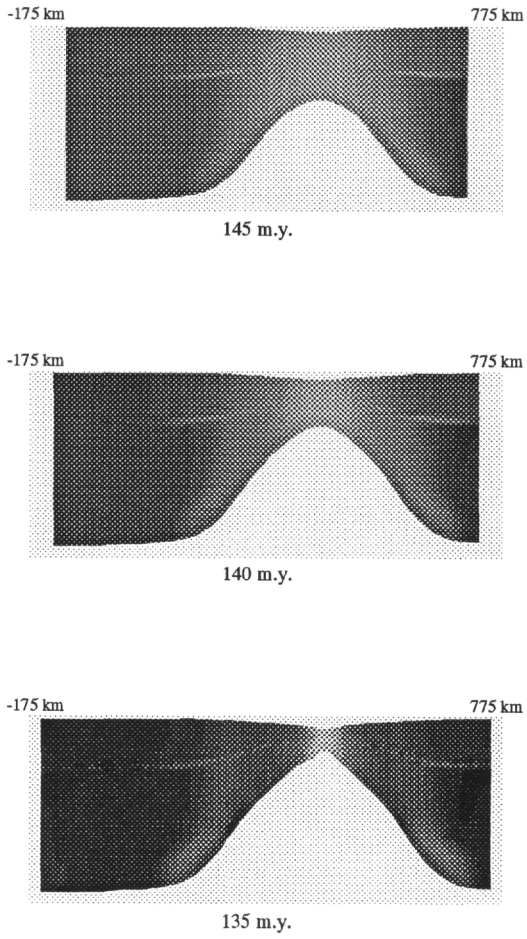

Figure 14. Strain rate plot for the model, showing the final necking of the lithosphere. Grays range from $\log_{10}$ (strain rate) of -14.9 (black) to -9.8 (white). The light background delineates the maximum width (950 km) and original thickness of the model (124.5 km).

This last issue notwithstanding, of all the models we tried—by varying crustal thickness, width of crustal and mantle weaknesses, Moho slope, constant-temperature boundary condition, and different constant heat-flow boundary conditions—this model provides the most accurate fit to the crustal profile and the subsidence. If it is indeed true that the driving forces of extension between North America and Iberia paused for almost 50 m.y., the model here suggests that the original crustal welt must have been narrow, and the amount of the extension during the first phase must have been minimal. Both implications are difficult to verify: the original crust has been obliterated by the extension we are examining, and the majority of first-phase synrift sediments accessible only through seismic surveys. We do not intend to imply that this model is the unique solution to the rifting between Newfoundland and Iberia; it is simply one possible model that fits the observations better than any other model we considered. Nevertheless, any future attempt to model spreading between Newfoundland and Iberia must consider the effects of the resting phase that separates the two.

MAGMATISM IN THE DYNAMIC RIFTING MODELS

A number of workers have discussed the issue of magmatism at rift zones (Foucher et al., 1982; McKenzie and Bickle, 1988; White and McKenzie, 1989; White, 1993). As pointed out earlier, the Newfoundland and Iberian Margins display little rift-related volcanism and are thus labeled "nonvolcanic." It was our intention to estimate the amount of magma generated by the foregoing models.

Like Harry and Sawyer (1992b), we considered only partial melt generated within the upwelling asthenosphere (that is, material that lies "underneath" the finite element mesh); the mantle rock within the mesh is too cold to produce any magma. We next needed to consider the temperature of the underlying asthenospheric material. As discussed earlier by Bassi et al. (1993), the heat-flow bottom boundary condition allows the lithosphere to cool too fast; therefore, we attempted to imitate their temperature boundary conditions in order to generate a more realistic magma generation model. For each vertical slice across each model, and at every 5 m.y. throughout each model,

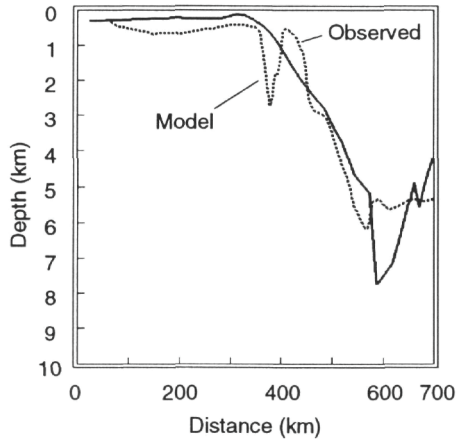

Figure 15. Elevation profile of the surface of the model at time 130 Ma (+100 Ma; the last executed step) plotted beside the observed sediment-stripped depth-to-basement. The left side represents Newfoundland, and the right side represents the Iberian Margin. The point of greatest necking appears at about 600 km in this figure. The x-axis values are arbitrary and are meant only to indicate horizontal scale.

we computed the geotherm down to the original model depth (about 125 km in all cases). This was done by using a one-dimensional finite difference routine to simulate the conduction of heat through the lithosphere. (The temperatures in this model were computed independently of those used in the dynamic models. The effect of this revision was higher, more realistic temperatures.) We maintained the surface of the model at 0°C and a constant 1333°C at a depth of 125 km.

At each time step, as the lithosphere thinned, we added an amount of "fresh" asthenosphere material at 1333°C at the bottom, for which the thickness was equal to the amount of thinning. This scheme approximates the upwelling of asthenosphere into the space left by thinning lithosphere and the subsequent accretion of that material onto the base of the lithosphere. Beneath an actual rift, this material may continue to convect, and thus maintain elevated temperatures, instead of accreting to the lithosphere. This possibility suggests that the temperature scheme used here may still underestimate temperatures in the space down to 125 km depth. However, the scheme used here approximates the lower lithosphere processes better than the schemes available in the dynamic models.

Once we had calculated a geotherm for every location and time in each model, we computed the pressure imposed by the overburden. Hence, having a pressure and temperature at every point, we used McKenzie and Bickle's (1988) relations to compute the percentage of partial melt generated at each point. Integrating the result over each vertical slice yielded the thickness of magma that would be erupted on the surface at the top of each slice at each point in time (assuming the melt travelled directly and immediately upward).

We applied this analysis to every model (including those not discussed here). In each case, no magma was generated at any time at any location throughout the model run. For the rates of rifting modeled here (10 km/m.y. and less), the mantle cooled too quickly to allow asthenospheric material to decompress sufficiently to create melt. Because even our fastest model did not produce any melt using this method, it can be safely concluded that the slower models—and the actual margins they may represent—were not close to producing any partial melt.

This conclusion is consistent with the observations from the Newfoundland and Iberian Margins, which show no significant magmatism at the surface. Furthermore, the rate of rifting has a decided impact on whether or not, and how much, melt will be generated at rifting margins. In addition to considering the initial temperature of the asthenosphere and the presence or absence of a "mantle plume" beneath a rifting margin, future researchers interested in examining melt generation at rifting margins should consider the rate of rifting as well. Instead of considering only "hot and cold rifts" (White, 1993), we should also consider "fast" and "slow" rifts in the magma-forming process.

CONCLUSIONS

Through dynamic modeling of multiphase rifting in general, and of the conjugate margins in particular, we have determined the following:

1. Upper mantle extension localizes where the Moho is hottest. This observation explains lateral migration of the locus of rifting as well as the rifting style produced by multiphase rifting. In most cases, the site of the original rift will not be favored for extension when stretching resumes, because the Moho will have been elevated by the first rifting phase and subsequently cooled. The magnitude of this effect is dependent on the thermal regime at the base of the lithosphere and on the amount of sedimentation.
2. The first phase of rifting between Newfoundland and Iberia (late Triassic to Early Jurassic) was probably minor; most of the extension occurred in the second phase (Late Jurassic to Early Cretaceous). Rifting took place in the same location during both rift phases; if the first rifting phase had elevated and cooled the Moho—thus strengthening the lithosphere—the second phase probably would have occurred elsewhere. In addition, the estimated amount of extension (about 400 km over an original width of about 600 km) and the duration of extension (35 Ma in the last rifting phase) appear reasonably close to the correct amounts. Although the dynamic model of the Newfoundland-Iberia conjugate margins is not a unique solution, it provides the best fit to the observations on those margins.
3. The present models do not predict the existence of a 400-km-wide zone of highly thinned continental crust. We have not yet seen a model created by the FEM and by rheologies used here that results in such a feature. This shortcoming may be due to the limitations of the modeling method. Nevertheless, based on the results of the models presented here, it would seem more likely that the Newfoundland Basin and Iberia Abyssal Plain are not underlain by crust of continental affinity. This, in turn, suggests that the ocean/continent boundary is in the vicinity of the shelf break on both margins.
4. No magmatism is predicted by the model. This observation is consistent with the lack of rift-related igneous activity on the Newfoundland and Iberian Margins. The lack of volcanism is probably the result of both a low initial asthenosphere temperature and the slow rate of rifting. Because it seems likely that the Newfoundland Basin and Iberia Abyssal Plain are underlain neither by continental crust nor by igneous crust created by initial seafloor spreading, it may be that these areas are underlain by mantle rock slowly unroofed by extension of the overlying continental crust. This conclusion can only be described as highly speculative, however, since at this time we lack any other evidence to support it.

ACKNOWLEDGMENTS

DLT wishes to thank the Amoco Foundation for financial support of his research while at Rice University, and Amoco Corporation management for their permission to publish this paper.

REFERENCES

Austin, J.A., Jr., Tucholke, B.E., and Uchupi, E., 1989. Upper Triassic-lower Jurassic salt basin southeast of the Grand Banks. *Earth Planet. Sci. Lett.,* 92:357-370.

Banda, E., 1988. Crustal parameters in the Iberian Peninsula. *Phys. Earth Planet. Inter.,* 51:222-225.

Bassi, G., 1991. Factors controlling the style of continental rifting: insights from numerical modeling. *Earth Planet. Sci. Lett.,* 105:430-452.

Bassi, G., Keen, C.E., and Potter, P., 1993. Contrasting styles of rifting: models and examples from the eastern Canadian margin. *Tectonics,* 12:639-655.

Boillot, G., Recq, M., Winterer, E.L., Meyer, A.W., Applegate, J., Baltuck, M., Bergen, J.A., Comas, M.C., Davies, T.A., Dunham, K., Evans, C.A., Girardeau, J., Goldberg, G., Haggerty, J., Jansa, L.F., Johnson, J.A., Kasahara, J., Loreau, J.P., Luna-Sierra, E., Moullade, M., Ogg, J., Sarti, M., Thurow, J., and Williamson, M., 1987. Tectonic denudation of the upper mantle along passive margins: a model based on drilling results (ODP Leg 103, Western Galicia Margin, Spain). *Tectonophysics,* 132:335-342.

Braun, J., and Beaumont, C, 1987. Styles of continental rifting: results from dynamic models of lithospheric extension. *In* Beaumont, C., and Tankard, A.J. (Eds.), *Sedimentary Basins and Basin-Forming Mechanisms.* CSPGMem., 12:241-258.

———, 1989a. A physical explanation of the relation between flank uplifts and the break up unconformity at rifted continental margins. *Geology,* 17:760-764.

———, 1989b. Contrasting styles of lithospheric extension: implications for differences between the Basin and Range province and rifted continental margins. *In* Tankard, A.J., and Balkwill, H.R. (Eds.), *Extensional Tectonics and Stratigraphy of the North Atlantic Margins.* AAPG Mem., 46:53-79.

Byerlee, J., 1978. Friction of rocks. *Pure Appl. Geophys.,* 116:615-626.

Chéry, J., Lucazeau, F., Daignières, M., and Vilotte, J.-P., 1990. The deformation of continental crust in extensional zones: a numerical approach. *In* Pinet, B., and Bois, C. (Eds.), *The Potential of Deep Seismic Profiling for Hydrocarbon Exploration:* Paris (Éditions Technip), 35-44.

Chopra, P.N., and Paterson, M.S., 1981. The experimental deformation of dunite. *Tectonophysics,* 78:453-473.

Cordoba, D., Banda, E., and Ansorge, J., 1988. P-wave velocity-depth distribution in the Hercynian crust of northwest Spain. *Phys. Earth Planet. Inter.,* 51:235-248.

Dunbar, J.A., and Sawyer, D.S., 1988. Continental rifting at pre-existing lithospheric weaknesses. *Nature,* 333:450-452.

———, 1989. How preexisting weaknesses control the style of continental breakup. *J. Geophys. Res.,* 94:7278-7292.

England, P., 1983. Constraints on extension of continental lithosphere. *J. Geophys. Res.,* 88:1145-1152.

Foucher, J.-P., Le Pichon, X., and Sibuet, J.-C., 1982. The ocean-continent transition in the uniform lithospheric stretching model: role of partial melting in the mantle. *Philos. Trans. R. Soc. London A,* 305:27-43.

Grant, A.C., Jansa, L.F., McAlpine, K.D., and Edwards, A., 1988. Mesozoic-cenozoic geology of the eastern margin of the Grand Banks and its relation to the Galicia Bank. *In* Boillot, G., Winterer, E.L., et al., *Proc. ODP, Sci. Results,* 103: College Station, TX (Ocean Drilling Program), 787-808.

Groupe Galice, 1979. The continental margin off Galicia and Portugal: acoustical stratigraphy, dredge stratigraphy, and structural evolution. *In* Sibuet, J.-C., Ryan, W.B.F., et al., *Init. Repts. DSDP,* 47 (Pt. 2): Washington (U.S. Govt. Printing Office), 633-662.

Hansen, F.D., and Carter, N.L., 1982. Creep of selected crustal rocks at 1000 MPa. *Eos,* 63:437. (Abstract)

———, 1983. Semibrittle creep of dry and wet Westerly granite at 1000 MPa. *Proc. 24th U.S. Symp. Rock Mechanics,* Texas A&M Univ., 429-447.

Harland, W.B., Armstrong, R.L., Cox, A.V., Craig, L.E., Smith, A.G., and Smith, D.G., 1990. *A Geologic Time Scale 1989:* Cambridge (Cambridge Univ. Press).

Harry, D.L., and Sawyer, D.S., 1992a. A dynamic model of lithospheric extension in the Baltimore Canyon Trough region. *Tectonics,* 11:420-436.

———, 1992b. Basaltic volcanism, mantle plumes, and the mechanics of rifting: the Paraná flood basalt province of South America. *Geology,* 20:207-210.

Hiscott, R.N., Wilson, R.C.L., Gradstein, F.M., Pujalte, V., García-Mondéjar, J., Boudreau, R.R., and Wishart, H.A., 1990. Comparative stratigraphy and subsidence history of Mesozoic rift basins of North Atlantic. *AAPG Bull.,* 74:60-76.

Keen, C.E., 1985. The dynamics of rifting: deformation of the lithosphere by active and passive driving forces. *Philos. Trans. R. Soc. London,* 80:95-120.

Keen, C.E, and Boutilier, R., 1990. Geodynamic modeling of rift basins: the syn-rift evolution of a simple half-graben. *In* Pinet, B., and Bois, C. (Eds.), *The Potential of Deep Seismic Profiling for Hydrocarbon Exploration:* Paris (Éditions Technip), 23-33.

Keen, C.E., Boutilier, R., de Voogd, B., Mudford, B., and Enachescu, M.E., 1987. Crustal geometry and extensional models for the Grand Banks, eastern Canada: constraints from deep seismic reflection data. *In* Beaumont, C., and Tankard, A.J. (Eds.), *Sedimentary Basins and Basin-Forming Mechanisms.* CSPG Mem., 12:101-115.

Keen, C.E., and de Voogd, B., 1988. The continent-ocean boundary at the rifted margin off eastern Canada: new results from deep seismic reflection studies. *Tectonics,* 7:107-124.

Keen, C E., Keen, M.J., Nichols, B., Reid, I., Stockmal, G.S., Colman-Sadd, S.P., O'Brien, S.J., Miller, H., Quinlan, G., Williams, H., and Wright, J., 1986. Deep seismic reflection profile across the northern Appalachians. *Geology,* 14:141-145.

Keen, C.E., Loncarevic, B.D., Reid, I., Woodside, J., Haworth, R.T., and Williams, H., 1990. Tectonic and geophysical overview. *In* Keen, M.J., and Williams, G.L. (Eds.), *Geology of the Continental Margin of Eastern Canada.* Geol. Can., 2:31-85.

Kusznir, N.J., and Ziegler, P.A., 1992. The mechanics of continental extension and sedimentary basin formation: a simple-shear/pure-shear flexural cantilever model. *Tectonophysics,* 215:117-131,

Lefort, J.-P., 1989. *Basement Correlation across the North Atlantic:* Berlin (Springer-Verlag).

Leinfelder, R.R., and Wilson, R.C.L., 1989. Seismic and sedimentologic features of Oxfordian-Kimmeridgian syn-rift sediments on the eastern margin of the Lusitanian Basin. *Geol. Rundsch.,* 78:81-104.

Malod, J.A., and Mauffret, A., 1990. Iberian plate motions during the Mesozoic. *Tectonophysics,* 184:261-278.

Masson, D.G., and Miles, P.R., 1984. Mesozoic seafloor spreading between Iberia, Europe and North America. *Mar. Geol.,* 56:279-287.

———, 1986. Development and hydrocarbon potential of Mesozoic sedimentary basins around margins of North Atlantic. *AAPG Bull.,* 70:721-729.

Mauffret, A., and Montadert, L., 1987. Rift tectonics on the passive continental margin off Galicia (Spain). *Mar. Pet. Geol.,* 4:49-70.

McKenzie, D., and Bickle, M.J., 1988. The volume and composition of melt generated by extension of the lithosphere. *J. Petrol.,* 29:625-679.

Meador, K.J., and Austin, J.A., Jr., 1988. A seismic comparison of the early stratigraphic evolution of conjugate passive continental margins: the Newfoundland/Flemish Basin and the Eastern Iberia Abyssal Plain south of Galicia Bank. *In* Boillot, G., Winterer, E.L., et al., *Proc. ODP, Sci. Results,* 103: College Station, TX (Ocean Drilling Program), 777-786.

Montenat, C., Guery, F., Jamet, M., and Berthou, Y.B., 1988. Mesozoic evolution of the Lusitanian Basin: comparison with the adjacent margin. *In* Boillot, G., Winterer, E.L., et al., *Proc. ODP, Sci. Results,* 103: College Station, TX (Ocean Drilling Program), 757-775.

Murillas, J., Mougenot, D., Boillot, G., Comas, M.C., Banda, E., and Mauffret, A., 1990. Structure and evolution of the Galicia Interior basin (Atlantic western Iberian continental margin). *Tectonophysics,* 184:297-319.

Parson, L.M., Masson, D.G., Pelton, C.D., and Grant, A.C., 1985. Seismic stratigraphy and structure of the east Canadian continental margin between 41 and 52°N. *Can. J. Earth Sci.,* 22:686-703.

Pitman, W.C., III, and Talwani, M., 1972. Sea-floor spreading in the North Atlantic. *Geol. Soc. Am. Bull.,* 83:619-646.

Reid, I.D., and Keen, C.E., 1990. Deep crustal structure beneath a rifted basin: results from seismic refraction measurements across the Jeanne d'Arc Basin, offshore eastern Canada. *Can. J. Earth Sci.,* 27:1462-1471.

Rowley, D.B., and Sahagian, D., 1986. Depth-dependent stretching: a different approach. *Geology,* 14:32-35.

Sawyer, D.S., 1985. Brittle failure in the upper mantle during extension of continental lithosphere. *J. Geophys. Res.,* 90:3021-3025.

Srivastava, S.P., Roest, W.R., Kovacs, L.C., Oakey, G., Levesque, S., Verhoef, J., and Macnab, R., 1990. Motion of Iberia since the Late Jurassic: results from detailed aeromagnetic measurements in the Newfoundland Basin. *Tectonophysics,* 184:229-260.

Srivastava, S.P., and Verhoef, J., 1992. Evolution of Mesozoic sedimentary basins around the North Central Atlantic: a preliminary plate kinematic solution. *In* Parnell, J. (Ed.), *Basins of the Atlantic Seaboard: Petroleum Geology, Sedimentology and Basin Evolution.* Geol. Spec. Publ. London, 62:397-420.

Srivastava, S.P., Verhoef, J., and Macnab, R., 1988. Results from a detailed aeromagnetic survey across the northeast Newfoundland margin. Part I. Spreading anomalies and relationship between magnetic anomalies and the ocean-continent boundary. *Mar. Pet. Geol.,* 5:306-323.

Steckler, M.S., and ten Brink, U.S., 1986. Lithospheric strength variations as a control on new plate boundaries: examples from the northern Red Sea. *Earth Planet. Sci. Lett.,* 79:120-132.

Sullivan, K.D., 1983. The Newfoundland Basin: ocean-continent boundary and Mesozoic seafloor spreading history. *Earth Planet. Sci. Lett.,* 62:321-339.

Tankard, A.J., and Welsink, H.J., 1987. Extensional tectonics and stratigraphy of Hibernia oil field, Grand Banks, Newfoundland. *AAPG Bull.,* 71:1210-1232.

———, 1988. Extensional tectonics, structural styles and stratigraphy of the Mesozoic Grand Banks of Newfoundland. *In* Manspeizer, W. (Ed.), *Triassic-Jurassic Rifting: Continental Breakup and the Origin of the Atlantic Ocean and Passive Margins* (Pt. A): Amsterdam (Elsevier), Devl. in Geotect., 22:129-165.

———, 1989. Mesozoic extension and styles of basin formation in Atlantic Canada. *In* Tankard, A.J., and Balkwill, H.R. (Eds.), *Extensional Tectonics and Stratigraphy of the North Atlantic Margins.* AAPG Mem., 46:175-195.

Tankard, A.J., Welsink, H.J., and Jenkins, W.A.M., 1989. Structural styles and stratigraphy of the Jeanne d'Arc Basin, Grand Banks of Newfoundland. *In* Tankard, A.J., and Balkwill, H.R. (Eds.), *Extensional Tectonics and Stratigraphy of the North Atlantic Margins.* AAPG Mem., 46:265-282.

Tett, D.L., 1993. The rifting history of the Newfoundland-Iberia conjugate margins: a geodynamic analysis [M.A. thesis]. Rice Univ., Houston, TX.

Tucholke, B.E., Austin, J.A., Jr., and Uchupi, E., 1989. Crustal structure and rift-drift evolution of the Newfoundland Basin. *In* Tankard, A.J., and Balkwill, H.R. (Eds.), *Extensional Tectonics and Stratigraphy of the North Atlantic Margins.* AAPG Mem., 46:247-263.

Tucholke, B.E., and Fry, V.A., 1985. Basement structure and sediment distribution in the Northwest Atlantic Ocean. *AAPG Bull.,* 69:2077-2097.

Tucholke, B.E., Houtz, R.E., and Ludwig, W.J., 1982. Sediment thickness and depth to basement in the western North Atlantic Ocean basin. *AAPG Bull.,* 66:1384-1395.

Tucholke, B.E., and Ludwig, W.J., 1982. Structure and origin of the J Anomaly ridge, western North Atlantic Ocean. *J. Geophys. Res.,* 87:9389-9407.

Welsink, H.J., Srivastava, S.P., and Tankard, A.J., 1989. Basin architecture of the Newfoundland continental margins and its relationship to ocean crust fabric during extension. *In* Tankard, A.J., and Balkwill, H.R. (Eds.), *Extensional Tectonics and Stratigraphy of the North Atlantic Margins.* AAPG Mem., 46:197-213.

White, R.S., 1993. Hot and cold rifts. *Eos,* 74:58.

White, R.S., and McKenzie, D., 1989. Magmatism at rift zones: the generation of volcanic continental margins and flood basalts. J. *Geophys. Res.,* 94:7685-7729.

Whitmarsh, R.B., Miles, P.R., and Mauffret, A., 1990. The ocean-continent boundary off the western continental margin of Iberia, I. Crustal structure at 40°30'N. *Geophys. J. Int.,* 103:509-531.

Whitmarsh, R.B., Pinheiro, L.M., Miles, P.R., Recq, M., and Sibuet, J.C., 1993. Thin crust at the western Iberia ocean-continent transition and ophiolites. *Tectonics,* 12:1230-1239.

Wilson, R.C.L., 1975. Atlantic opening and Mesozoic continental margin basins of Iberia. *Earth Planet. Sci. Lett.,* 25:33-43.

Wilson, R.C.L., Hiscott, R.N., Willis, M.G., and Gradstein, F.M., 1989. The Lusitanian Basin of west-central Portugal: Mesozoic and Tertiary tectonic, stratigraphic and subsidence history. *In* Tankard, A.J., and Balkwill, H.R. (Eds.), *Extensional Tectonics and Stratigraphy of the North Atlantic Margins.* AAPG Mem., 46:341-361.

Ziegler, P.A., 1989. Evolution of the North Atlantic—an overview. *In* Tankard, A.J., and Balkwill, H.R. (Eds.), *Extensional Tectonics and Stratigraphy of the North Atlantic Margins.* AAPG Mem., 46:111-129.

———, 1992. Plate tectonics, plate moving mechanisms and rifting. *Tectonophysics,* 215:9-34.

Date of initial receipt: 30 November 1994
Date of acceptance: 27 June 1995
149SR-247